Probing the origin of the stochastic GW background

Sachiko Kuroyanagi

(Nagoya University & IFT Madrid)

4 Sep 2019

Cosmo'19, Aachen

Stochastic GW background

Waveform

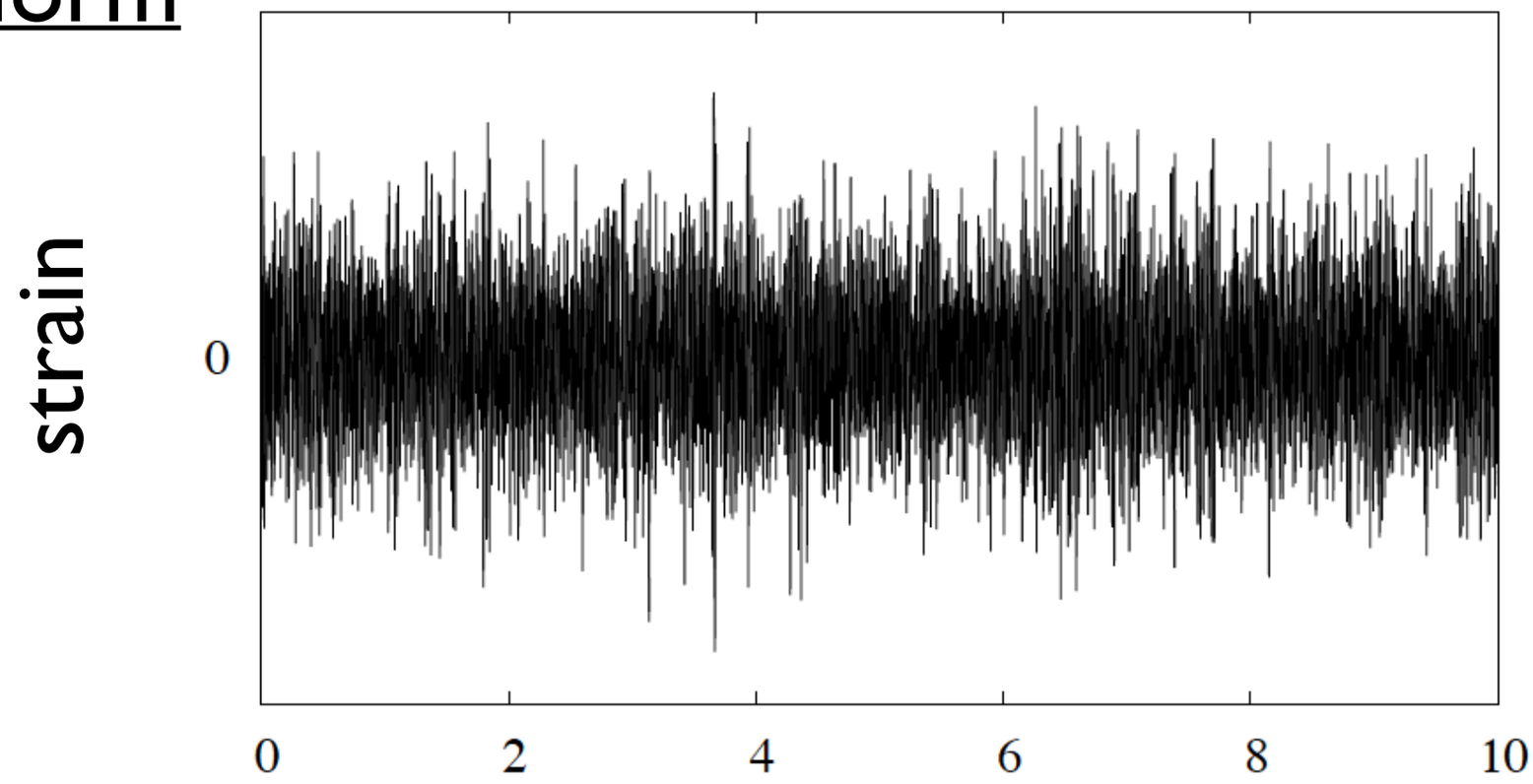

Continuous and random gravitational wave (GW) signal coming from all directions → very similar to noise

Generation mechanisms

Overlapped astrophysical GWs

interval of events $\Delta T < f^{-1}$

- Black hole binaries
- Neutron star binaries
- White dwarf binaries
- Supernovae

etc…

Cosmological GWs

generated in the early Universe

- Inflation
- Preheating
- Phase transitions
- Vector fields
- Cosmic strings

etc…

How can we determine the origin of the GW background?

→ go beyond the spectral amplitude
and use other types of information such as

1. Spectral shape

2. Polarization

3. Anisotropy

4. Popcorn noise

5. Non-Gaussianity

How to detect a stochastic background

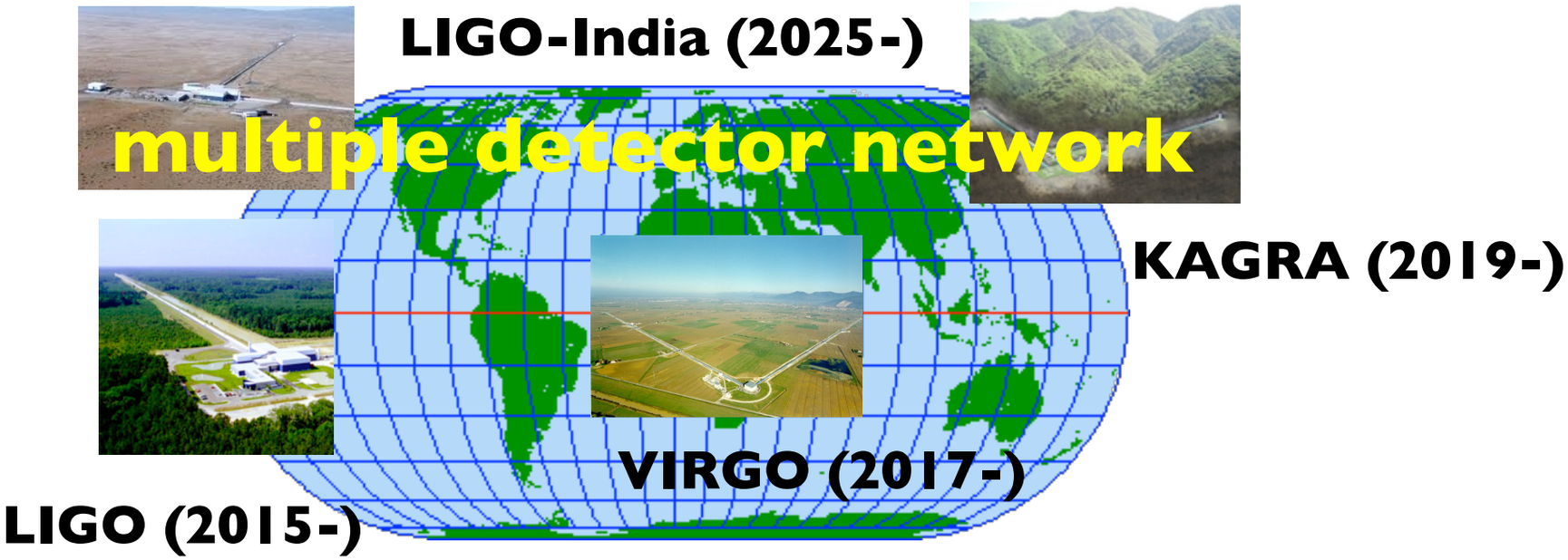

Cross Correlation

detector1 $s_1(t) = h(t) + n_1(t)$ ⟷ detector2 $s_2(t) = h(t) + n_2(t)$

s: observed signal
h: gravitational waves
n: noise

$$\langle S \rangle = \int_{-T/2}^{T/2} dt \, \langle s_1(t) s_2(t) \rangle$$

$$= \int_{-T/2}^{T/2} dt \, \langle h^2(t) + \underline{h(t)n_2(t) + n_1(t)h(t) + n_1(t)n_2(t)} \rangle$$

no correlations → 0

$$= \int_{-T/2}^{T/2} dt \, \underline{\langle h^2(t) \rangle}$$

GW signal

(for detectors at the same location)

Optimal filtering

B. Allen & J. Romano, PRD 59, 102001 (1999)

$$S := \int_{-T/2}^{T/2} dt \int_{-T/2}^{T/2} dt'\, s_1(t) s_2(t') \underline{Q(t,t')}$$

filter function

With the approximation $h \ll n$, the signal-to-noise ratio is

$$\mathrm{SNR}^2 = \frac{\mu^2}{\sigma^2} \approx \left(\frac{3H_0^2}{10\pi^2}\right)^2 T \frac{\left(\underline{\tilde{Q}}, \dfrac{\gamma(|f|)\Omega_{\mathrm{gw}}(|f|)}{|f|^3 P_1(|f|) P_2(|f|)}\right)^2}{(\underline{\tilde{Q}}, \underline{\tilde{Q}})}$$

$$(A,B) := \int_{-\infty}^{\infty} df\, A^*(f) B(f) P_1(|f|) P_2(|f|)$$

filter function in Fourier space

SNR is maximized when

$$\tilde{Q}(f) = \lambda \frac{\gamma(|f|)\Omega_{\mathrm{gw}}(|f|)}{|f|^3 P_1(|f|) P_2(|f|)}$$

Optimal filtering

B. Allen & J. Romano, PRD 59, 102001 (1999)

SNR is maximized when

$$\tilde{Q}(f) = \lambda \frac{\gamma(|f|)\Omega_{\rm gw}(|f|)}{|f|^3 P_1(|f|) P_2(|f|)}$$

Optimal filtering

B. Allen & J. Romano, PRD 59, 102001 (1999)

SNR is maximized when

$$\tilde{Q}(f) = \lambda \frac{\gamma(|f|)\Omega_{\rm gw}(|f|)}{|f|^3 P_1(|f|)P_2(|f|)}$$

$n(t) \to P_i(|f|)$: noise spectrum

observable:

$$s(t) = h(t) + n(t) \sim n(t)$$

$h \ll n$

→ **obtained from data**

Optimal filtering

B. Allen & J. Romano, PRD 59, 102001 (1999)

SNR is maximized when

$$\tilde{Q}(f) = \lambda \frac{\gamma(|f|)\,\Omega_{\rm gw}(|f|)}{|f|^3 P_1(|f|) P_2(|f|)}$$

$h(t) \to \Omega_{\rm gw}(|f|)$: GW spectrum

→ **unknown**

→ **We prepare**
a template bank
of spectral shape

$n(t) \to P_i(|f|)$: noise spectrum

observable:

$$s(t) = h(t) + n(t) \sim n(t)$$

$h \ll n$

→ **obtained from data**

Optimal filtering

B. Allen & J. Romano, PRD 59, 102001 (1999)

SNR is maximized when

$$\tilde{Q}(f) = \lambda \frac{\gamma(|f|)\,\Omega_{\rm gw}(|f|)}{|f|^3 P_1(|f|) P_2(|f|)}$$

overlap reduction function
determined by detector response

$h(t) \to \Omega_{\rm gw}(|f|)$: GW spectrum

→ **unknown**

→ **We prepare**
a template bank
of spectral shape

$n(t) \to P_i(|f|)$: noise spectrum

observable:

$$s(t) = h(t) + n(t) \sim n(t)$$

$h \ll n$

→ **obtained from data**

Detector response

Sensitivity of an interferometer depends on
source location and **polarization**

observable: $s(t) = \underline{F(\hat{\Omega})} h(t) + n(t)$

response function

$\hat{\Omega}$: direction of GW propagation

+ mode **× mode**

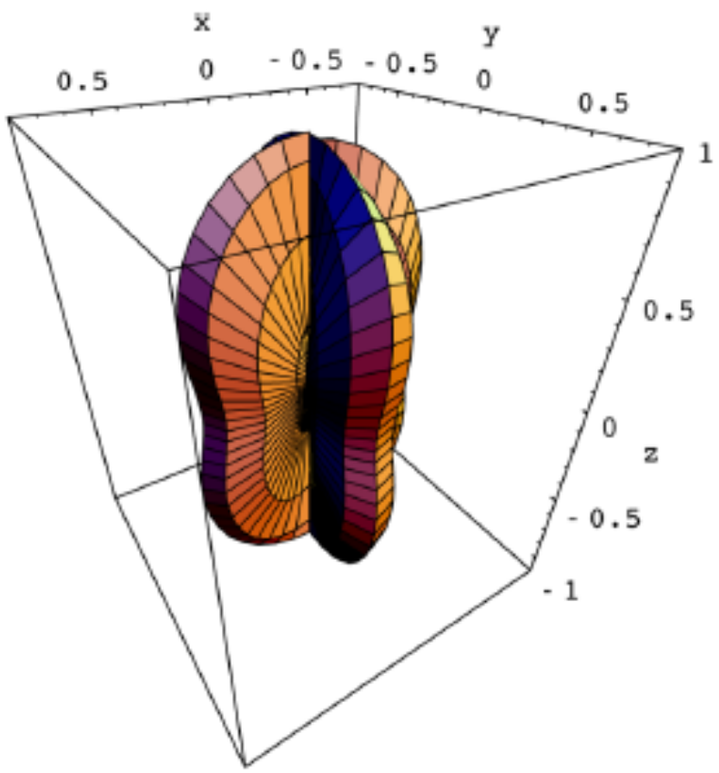

detector arms

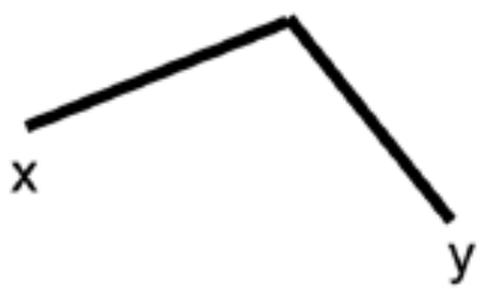

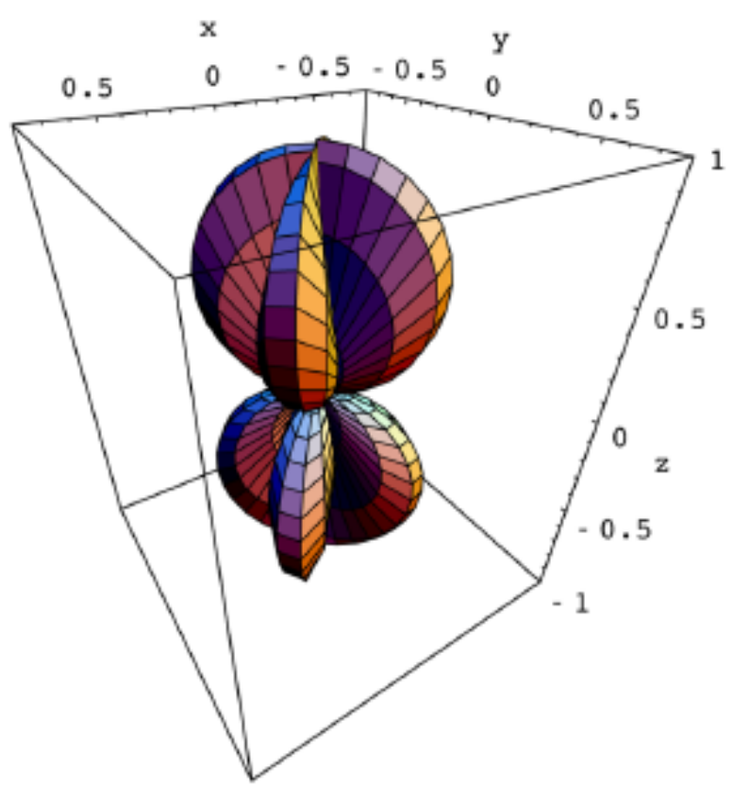

Figure from A. Nishizawa et al. PRD 79, 082002 (2009)

Overlap reduction function

For a stochastic GW background, we construct

$$\gamma_{IJ}^{T}(f) \equiv \frac{5}{2} \int_{S^2} \frac{d\hat{\mathbf{\Omega}}}{4\pi} e^{2\pi i f \hat{\Omega} \cdot \Delta\vec{X}/c} (F_I^+ F_J^+ + F_I^\times F_J^\times)$$

integration over the whole sky

separation of detectors

response function

I and J denote different detectors

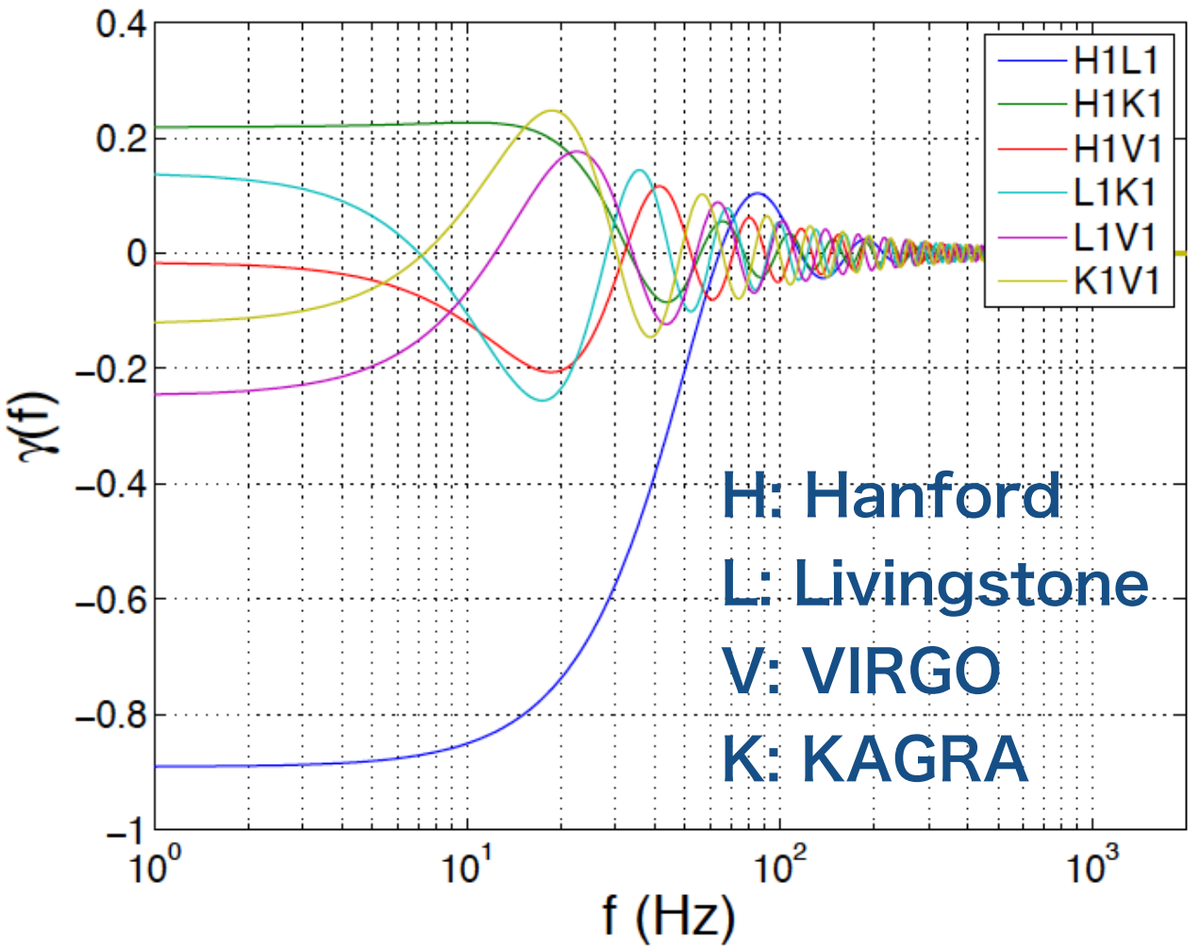

→ represents the amount of preserved correlation between two detectors

E. Thrane & J. D. Romano,
PRD 88, 124032 (2013)

1. Spectral shape

GW background is searched by changing
spectral shape template

filter function

$$\tilde{Q}(f) = \lambda \frac{\gamma(|f|)\Omega_{\rm gw}(|f|)}{|f|^3 P_1(|f|) P_2(|f|)}$$

usually parametrized by
a single power law

$$\Omega_{\rm GW}(f) = \Omega_\alpha \left(\frac{f}{f_{\rm ref}}\right)^\alpha$$

$f_{\rm ref} = 25{\rm Hz}$

LIGO & Virgo Collaboration, PRL 118, 121101 (2017)

→ but many models of GW background
predict a peaked shape

Template search: Example

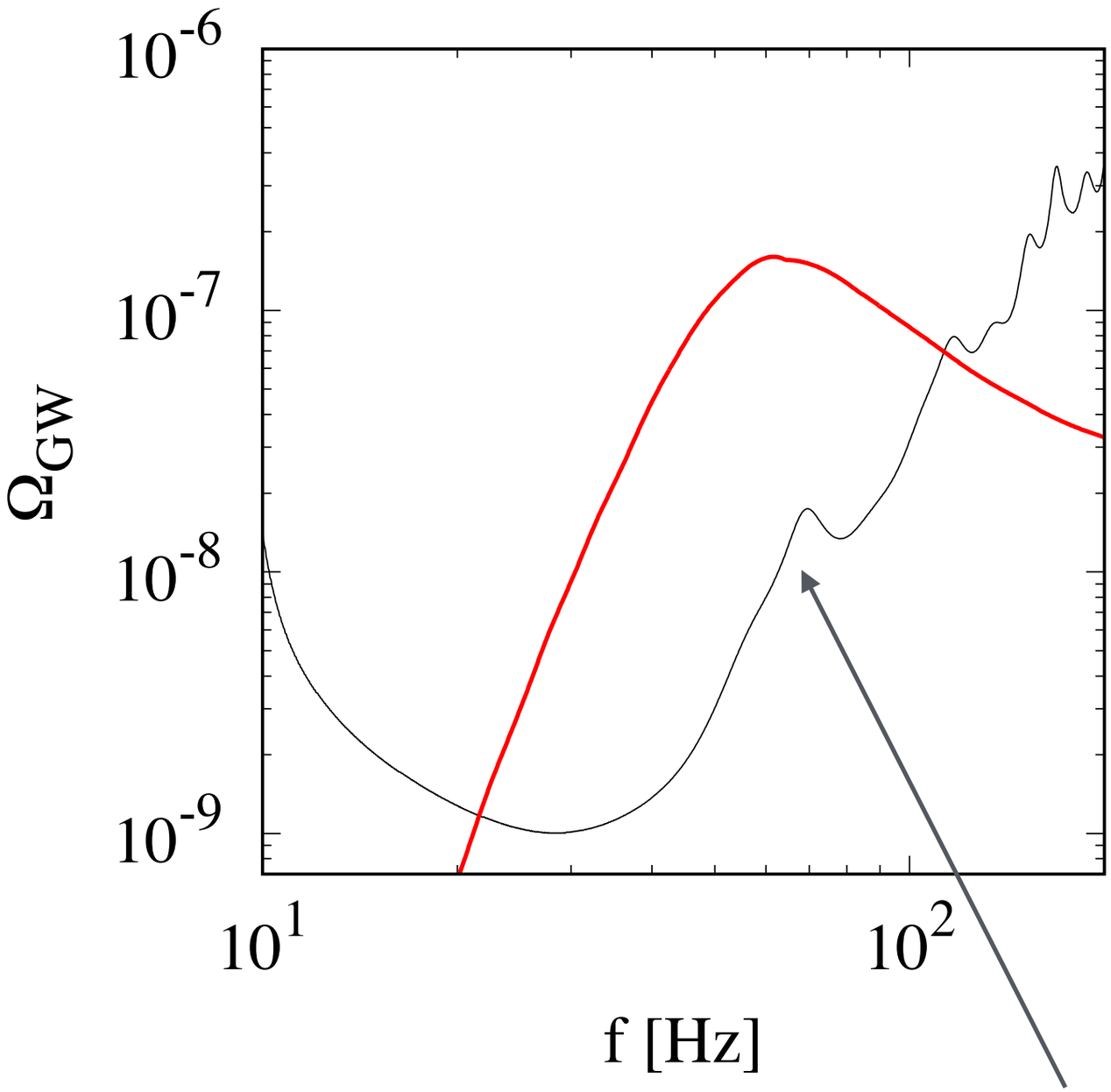

← true signal

GWB from superradiant instabilities
(ultralight scalar fields
around spinning black holes)

Brito et al. PRL 119, 131101 (2017)

LIGO+ VIRGO+KAGRA design sensitivity

Template search: Example

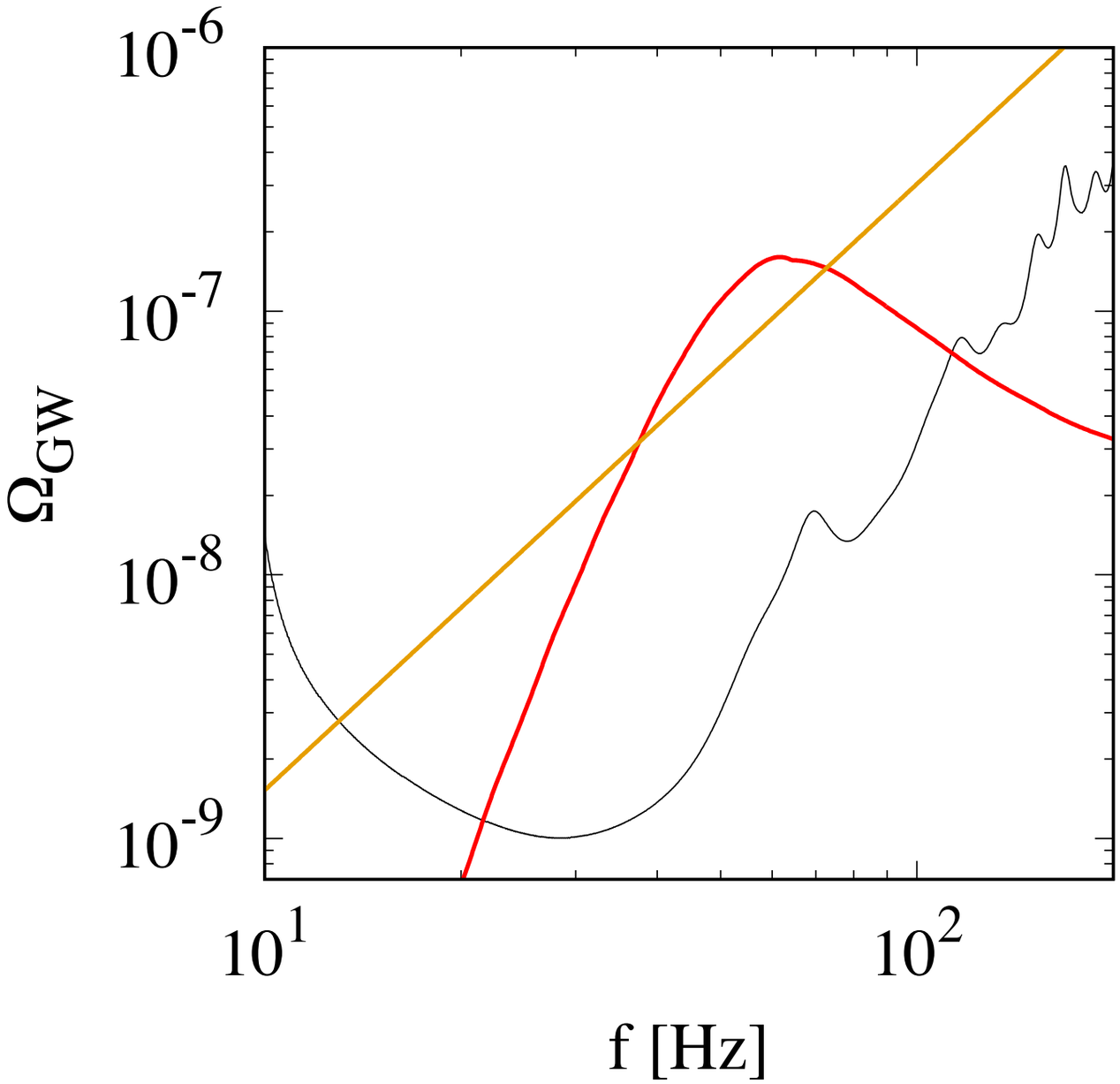

← single power-law template

$$\Omega_{\rm GW}(f) = \Omega_\alpha \left(\frac{f}{f_{\rm ref}}\right)^\alpha$$

$f_{\rm ref} = 25{\rm Hz}$

Best-fit values

$\alpha = 2.3$

$\Omega_\alpha = 1.25\times10^{-8}$

SNR=70.7, $\delta\chi^2$=1440

Template search: Example

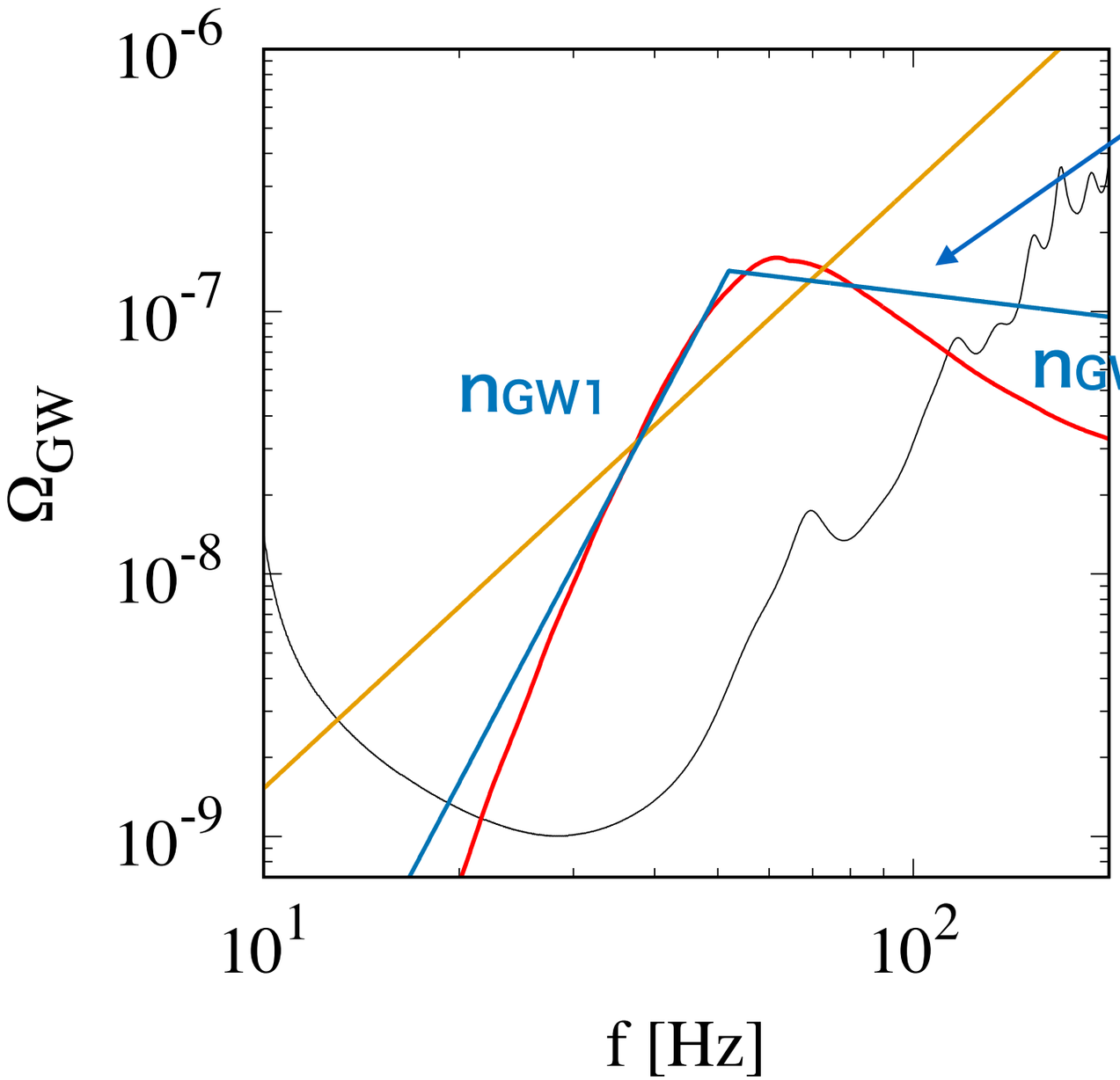

broken power-law template

$$\Omega_{\mathrm{GW}*}\left(\frac{f}{f_*}\right)^{n_{\mathrm{GW1}}} \quad \text{for} \quad f < f_*$$

$$\Omega_{\mathrm{GW}*}\left(\frac{f}{f_*}\right)^{n_{\mathrm{GW2}}} \quad \text{for} \quad f > f_*$$

Best-fit values

n_{GW1}=4.7　n_{GW2}=-0.3

$\Omega_{GW^*} = 1.43\times10^{-7}$

f_*=52[Hz]

SNR=80.0,　$\delta\chi^2$=47.4

S. Kuroyanagi, T. Chiba & T. Takahashi, JCAP11(2018)038

Template search: Example

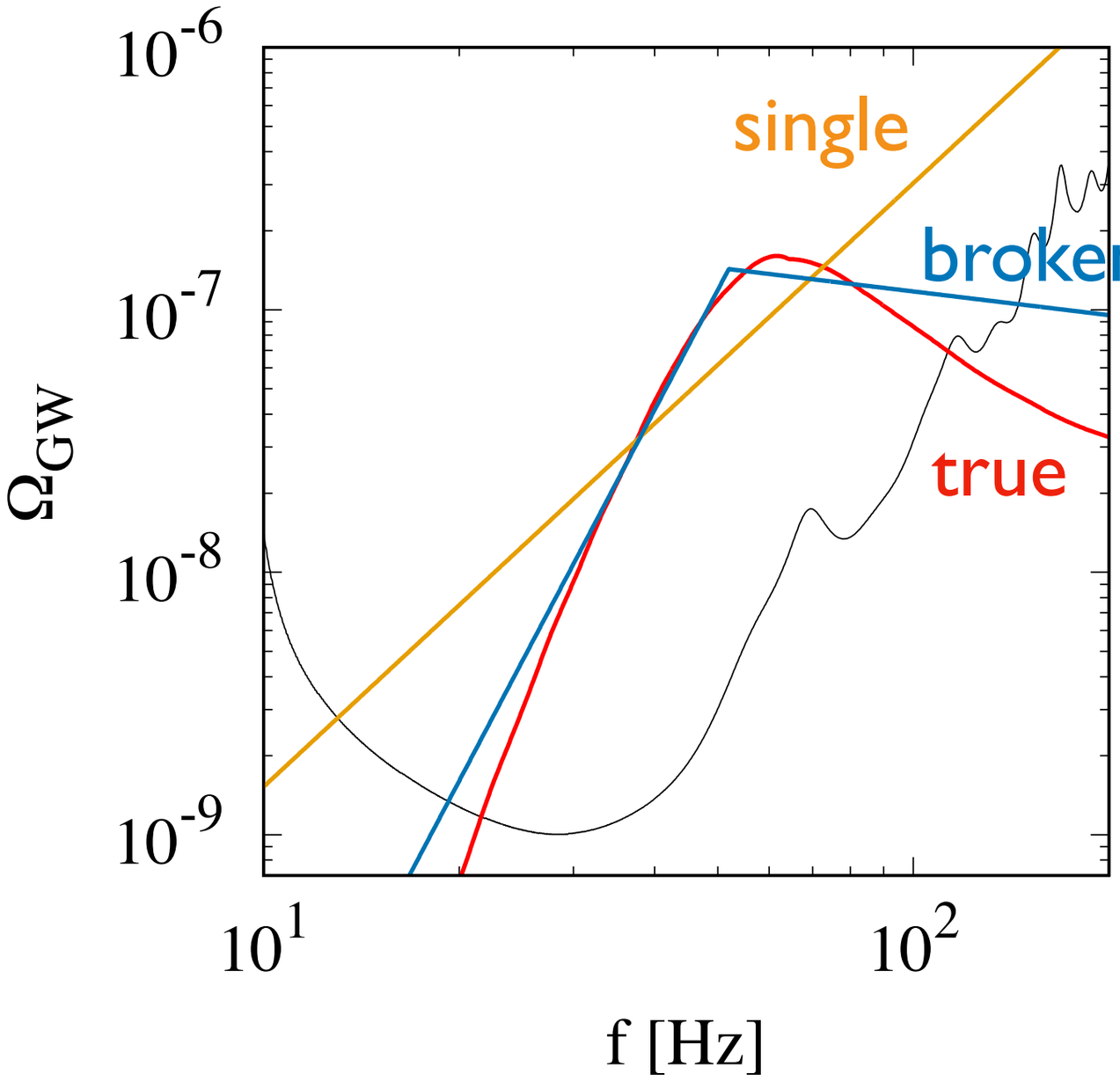

Single power law

SNR=70.7, $\delta\chi^2$=1440

Broken power law

SNR=80.0, $\delta\chi^2$=47.4

(cf. SNR=80.3 with perfectly matched template)

~10% loss of SNR for single power law

$\delta\chi^2$ improves a lot with a broken power law

S. Kuroyanagi, T. Chiba & T. Takahashi, JCAP11(2018)038

n_{GW1} & n_{GW2} for different mechanisms

source	$n_{\rm GW1}$	$n_{\rm GW2}$	f_* [Hz]	$\Omega_{\rm GW}$
Phase transition (bubble collision)	2.8	-2	$\sim 10^{-5}\left(\frac{f_{\rm PT}}{\beta}\right)\left(\frac{\beta}{H_{\rm PT}}\right)\left(\frac{T_{\rm PT}}{100\ {\rm GeV}}\right)$	$\sim 10^{-5}\left(\frac{H_{\rm PT}}{\beta}\right)^2\left(\frac{\kappa_\phi\alpha}{1+\alpha}\right)^2\left(\frac{0.11v_w^3}{0.42+v_w^2}\right)$
Phase transition (turbulence)	3	$-5/3$	$\sim 3\times10^{-5}\left(\frac{1}{v_w}\right)\left(\frac{\beta}{H_{\rm PT}}\right)\left(\frac{T_{\rm PT}}{100\ {\rm GeV}}\right)$	$\sim 3\times10^{-4}\left(\frac{H_{\rm PT}}{\beta}\right)\left(\frac{\kappa_{\rm turb}\alpha}{1+\alpha}\right)^{3/2}v_w$
Phase transition (sound waves)	3	-4	$\sim 2\times10^{-5}\left(\frac{1}{v_w}\right)\left(\frac{\beta}{H_{\rm PT}}\right)\left(\frac{T_{\rm PT}}{100\ {\rm GeV}}\right)$	$\sim 3\times10^{-6}\left(\frac{H_{\rm PT}}{\beta}\right)\left(\frac{\kappa_v\alpha}{1+\alpha}\right)^2 v_w$
Preheating ($\lambda\phi^4$)	3	cutoff	$\sim 10^7$	$\sim 10^{-11}\left(\frac{g^2/\lambda}{100}\right)^{-0.5}$
Preheating (hybrid)	2	cutoff	$\sim \frac{g}{\sqrt{\lambda}}\lambda^{1/4}10^{10.25}$	$\sim 10^{-5}\left(\frac{\lambda}{g^2}\right)^{1.16}\left(\frac{v}{M_{\rm pl}}\right)^2$
Cosmic strings (loops 1)	$[1,2]$	$[-1,-0.1]$	$\sim 3\times10^{-8}\left(\frac{G\mu}{10^{-11}}\right)^{-1}$	$\sim 10^{-9}\left(\frac{G\mu}{10^{-12}}\right)\left(\frac{\alpha_{\rm loop}}{10^{-1}}\right)^{-1/2}$(for $\alpha_{\rm loop}\gg\Gamma G\mu$)
Cosmic strings (loops 2)	$[-1,-0.1]$	0	$\sim 3\times10^{-8}\left(\frac{G\mu}{10^{-11}}\right)^{-1}$	$\sim 10^{-9.5}\left(\frac{G\mu}{10^{-12}}\right)\left(\frac{\alpha_{\rm loop}}{10^{-1}}\right)^{-1/2}$(for $\alpha_{\rm loop}\gg\Gamma G\mu$)
Cosmic strings (infinite strings)	$[0,0.2]$	$[0,0.2]$	—	$\sim 10^{-[11,13]}\left(\frac{G\mu}{10^{-8}}\right)$
Domain walls	3	-1	$\sim 10^{-9}\left(\frac{T_{\rm ann}}{10^{-2}{\rm GeV}}\right)$	$\sim 10^{-17}\left(\frac{\sigma}{1{\rm TeV}^3}\right)^2\left(\frac{T_{\rm ann}}{10^{-2}{\rm GeV}}\right)^{-4}$
Self-ordering scalar fields	0	0	—	$\sim \frac{511}{N}\Omega_{\rm rad}\left(\frac{v}{M_{\rm pl}}\right)^4$
Self-ordering scalar + reheating	0	-2	$\sim 0.4\left(\frac{T_R}{10^7\ {\rm GeV}}\right)$	$\sim \frac{511}{N}\Omega_{\rm rad}\left(\frac{v}{M_{\rm pl}}\right)^4$
Magnetic fields	3	α_B+1	$\sim 10^{-6}\left(\frac{T_*}{10^2{\rm GeV}}\right)$	$\sim 10^{-16}\left(\frac{B}{10^{-10}{\rm G}}\right)$
Inflation+reheating	~ 0	-2	$\sim 0.3\left(\frac{T_R}{10^7\ {\rm GeV}}\right)$	$\sim 2\times10^{-17}\left(\frac{r}{0.01}\right)$
Inflation+kination	~ 0	1	$\sim 0.3\left(\frac{T_R}{10^7\ {\rm GeV}}\right)$	$\sim 2\times10^{-17}\left(\frac{r}{0.01}\right)$
Particle prod. during inf.	-2ϵ	$-4\epsilon(4\pi\xi-6)(\epsilon-\eta)$	—	$\sim 2\times10^{-17}\left(\frac{r}{0.01}\right)$
2nd-order (inflation)	1	drop-off	$\sim 7\times10^5\left(\frac{T_{\rm reh}}{10^9\ {\rm GeV}}\right)^{1/3}\left(\frac{M_{\rm inf}}{10^{16}\ {\rm GeV}}\right)^{2/3}$	$\sim 10^{-12}\left(\frac{T_{\rm reh}}{10^9\ {\rm GeV}}\right)^{-4/3}\left(\frac{M_{\rm inf}}{10^{16}\ {\rm GeV}}\right)^{4/3}$
2nd-order (PBHs)	2	drop-off	$\sim 4\times10^{-2}\left(\frac{M_{\rm PBH}}{10^{20}\ {\rm g}}\right)^{-1/2}$	$\sim 7\times10^{-9}\left(\frac{\mathcal{A}^2}{10^{-3}}\right)^2$
Pre-Big-Bang	3	$3-2\mu$	—	$\sim 1.4\times10^{-6}\left(\frac{H_s}{0.15M_{\rm pl}}\right)^4$

measurements of n_{GW1} and n_{GW2} can determine the origin

S. Kuroyanagi, T. Chiba & T. Takahashi, JCAP11(2018)038

How accurately can we measure the tilt?

Prediction by Fisher analysis for $n_{GW1} = 3$, $n_{GW2} = -2$

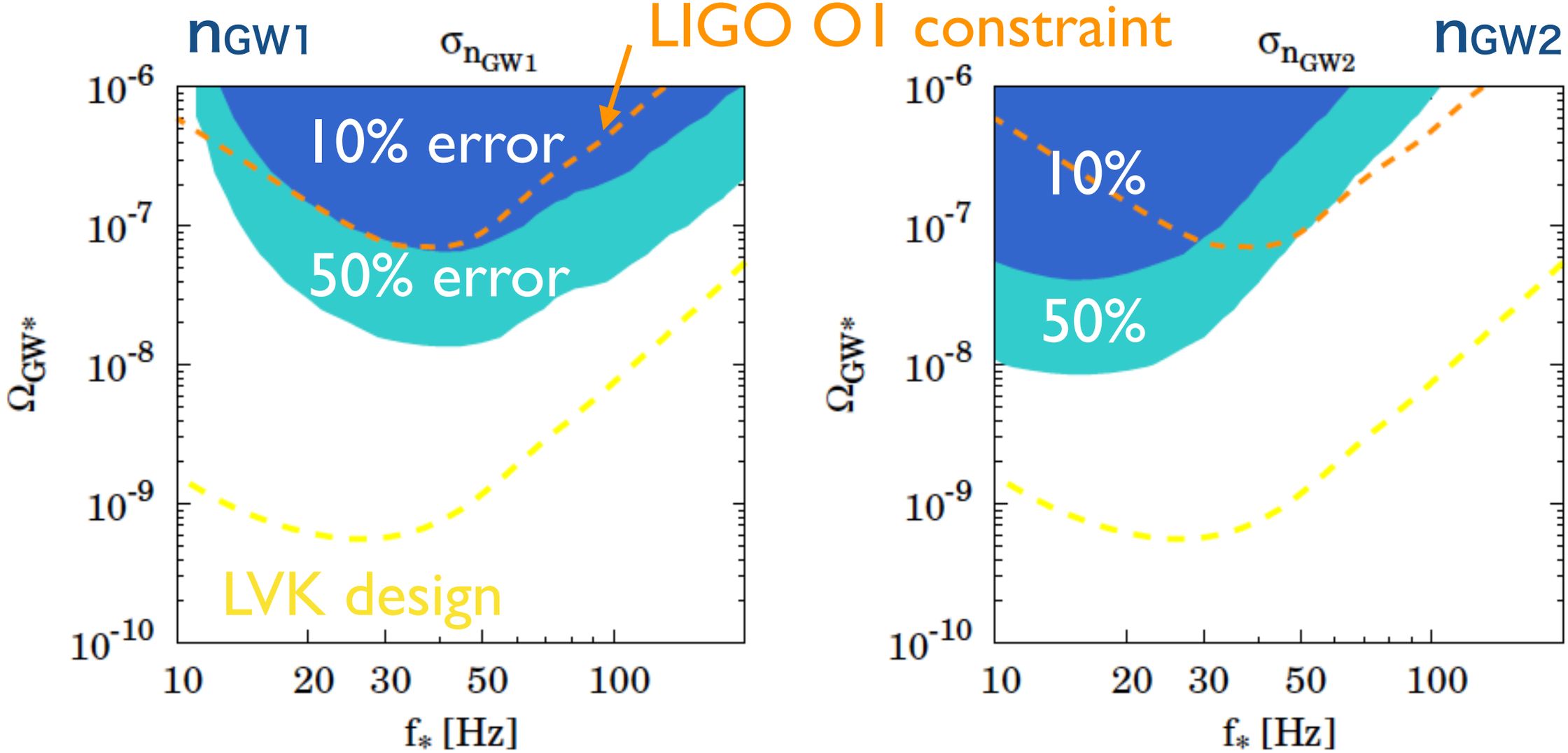

1. A large amplitude is necessary to measure the tilt
2. The error also depends on the peak position

S. Kuroyanagi, T. Chiba & T. Takahashi, JCAP11(2018)038

How accurately can we measure the tilt?

$\sigma_{n_{GW1},n_{GW2}} \propto SNR^{-1}$

$$\mathrm{SNR} \approx \frac{3H_0^2}{10\pi^2}\sqrt{T}\left[\int_{-\infty}^{\infty} df \frac{\gamma^2(|f|)\Omega_{\mathrm{gw}}^2(|f|)}{f^6 P_1(|f|)P_2(|f|)}\right]^{1/2}$$

signal

noise

→ integration of (signal/noise) in terms of frequency

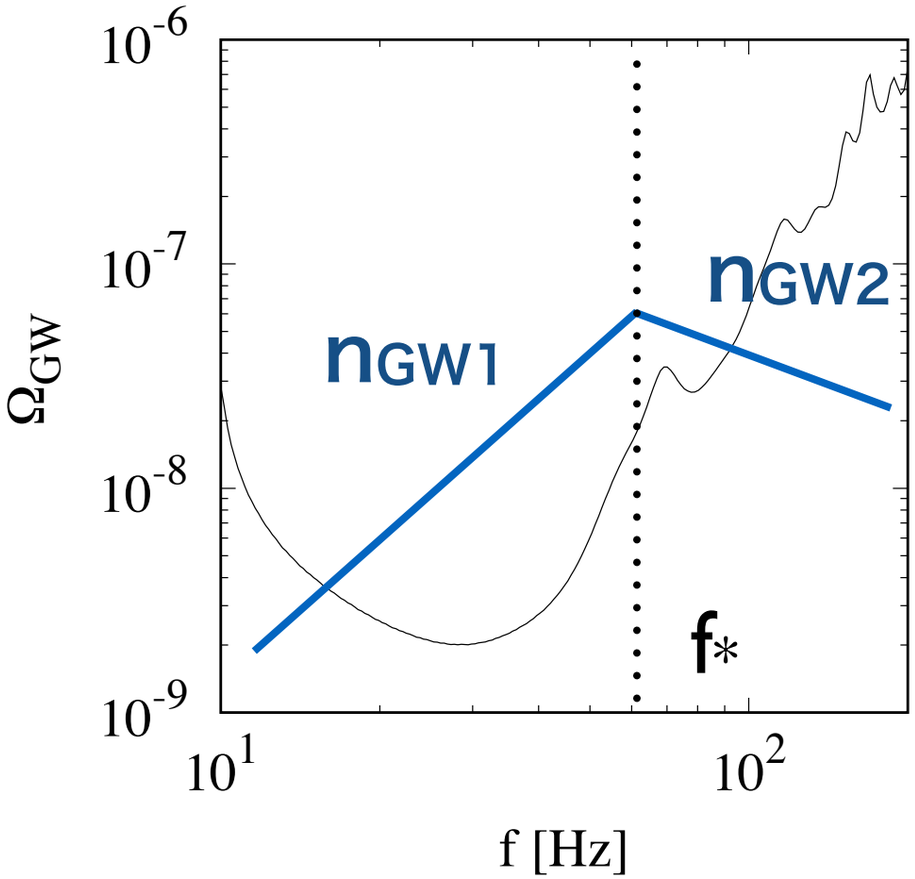

n_{GW1} is determined accurately

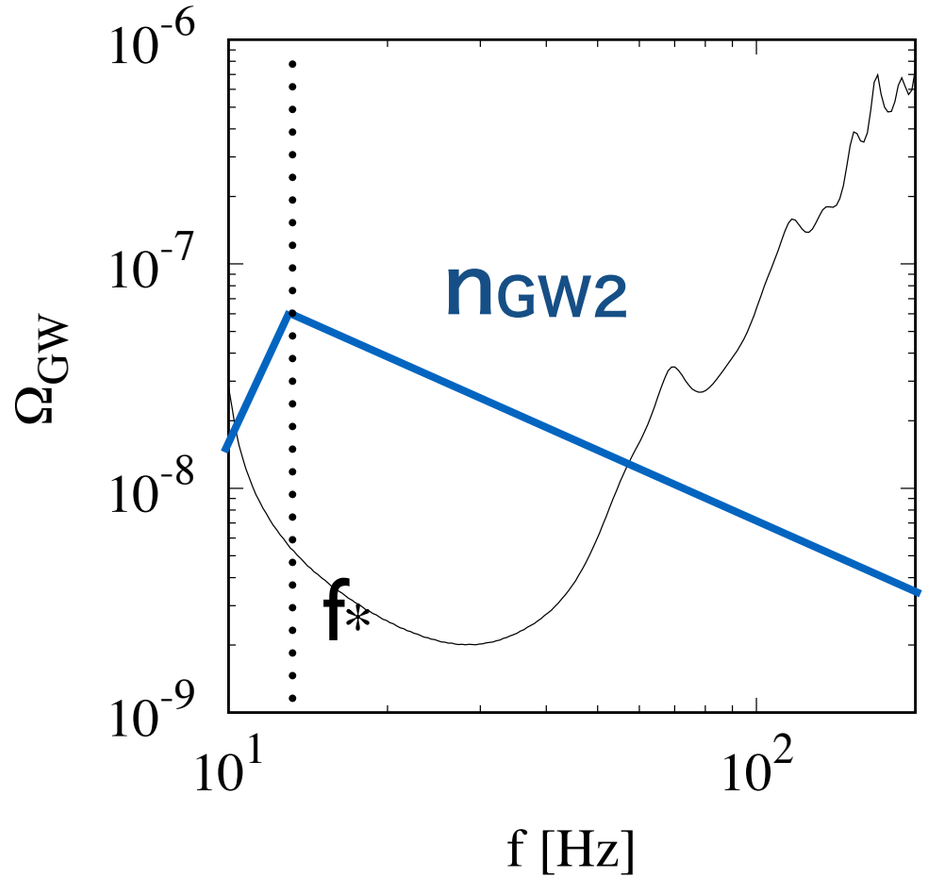

n_{GW2} is determined accurately

Multi-binning

Reconstruction of spectral shape (studied for LISA)

Spectral tilt is fitted in each bin

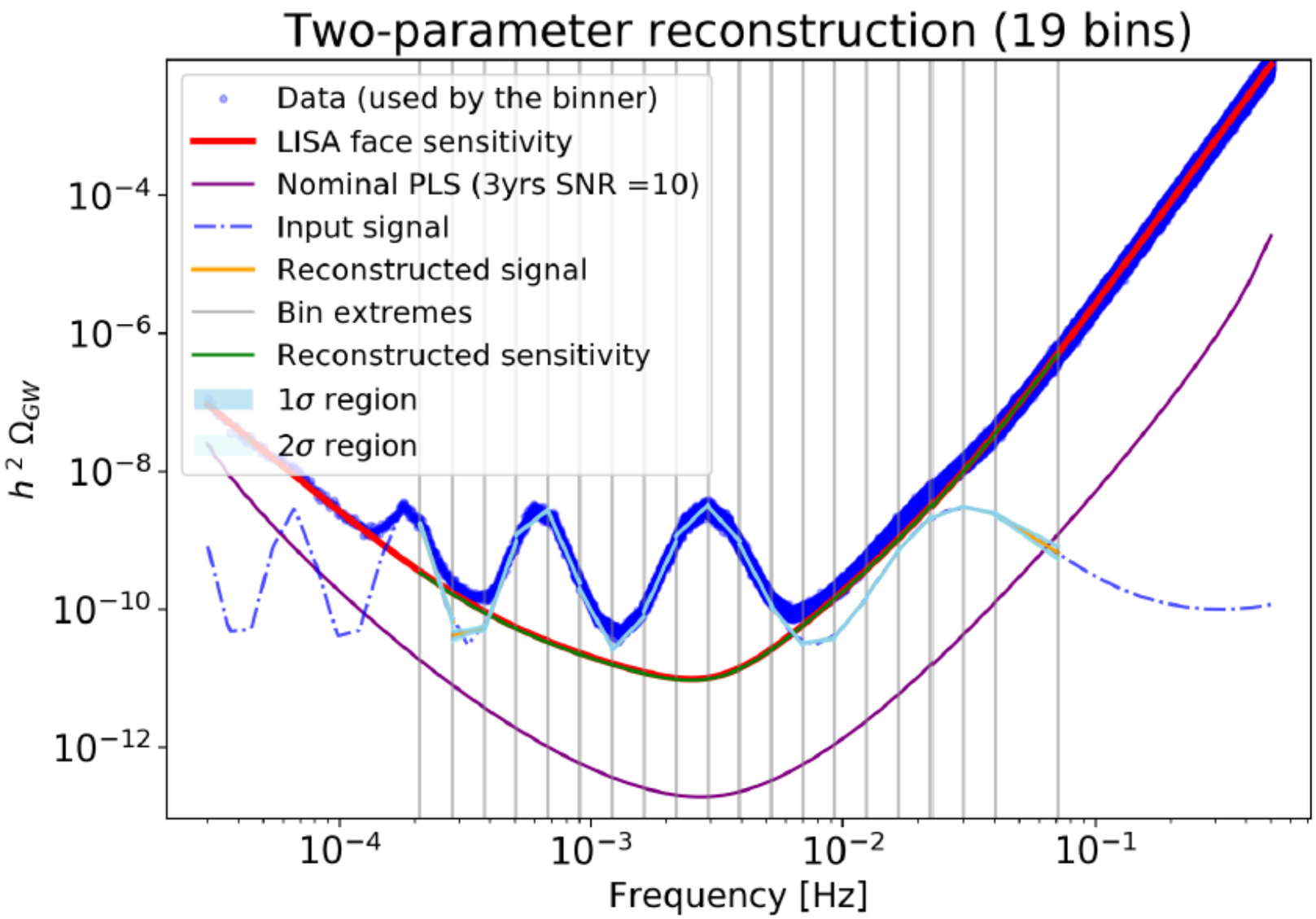

C. Caprini et al. (LISA Cosmology Working Group)
arXiv:1906.09244 [astro-ph.CO]

2. Polarization

Tensor | Scalar | Vector

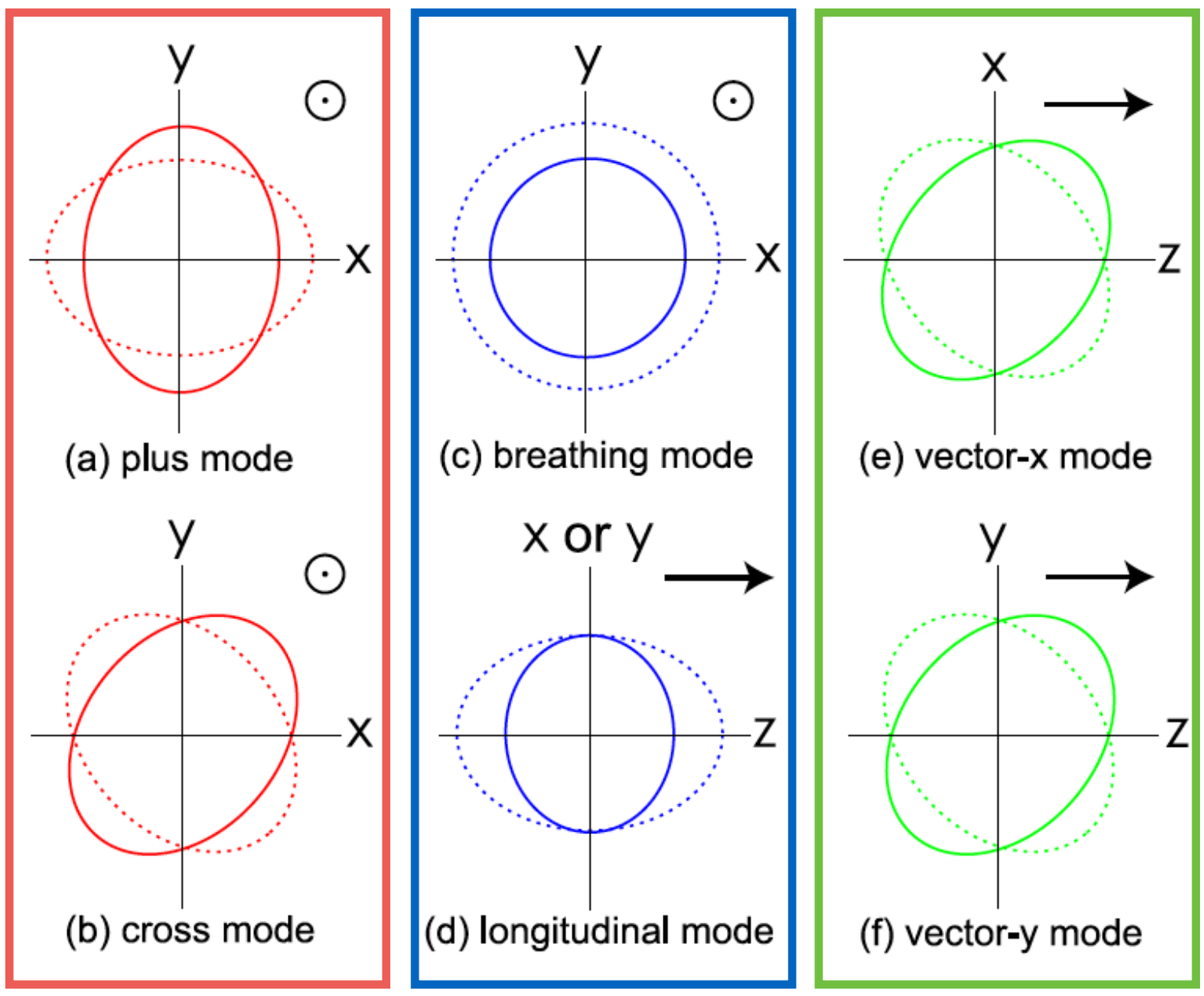

Linear + Circular modes → probe of non-GR

A. Nishizawa et al. PRD 79, 082002 (2009)

How can we detect polarization?

Detector response changes

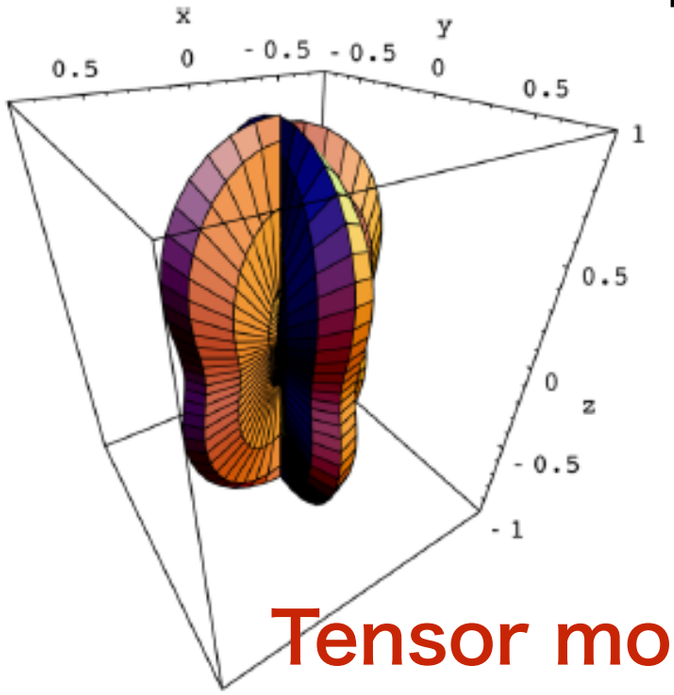

Tensor modes

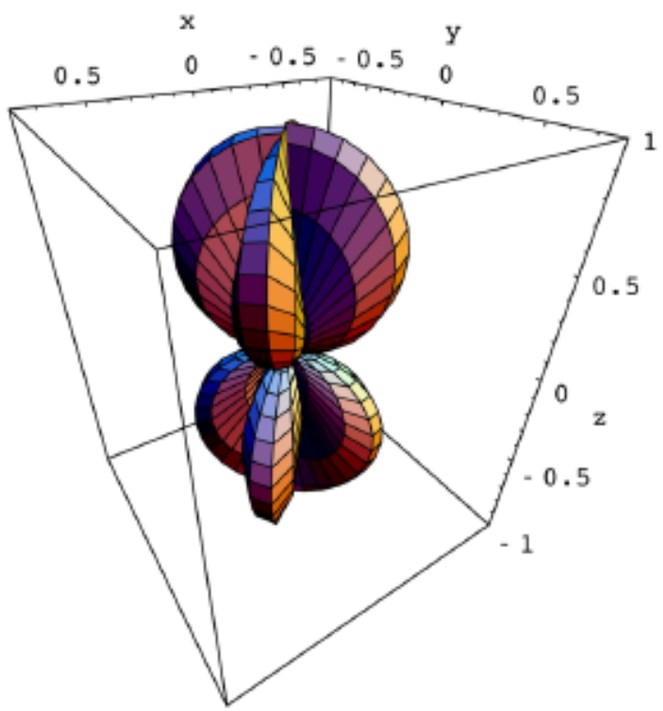

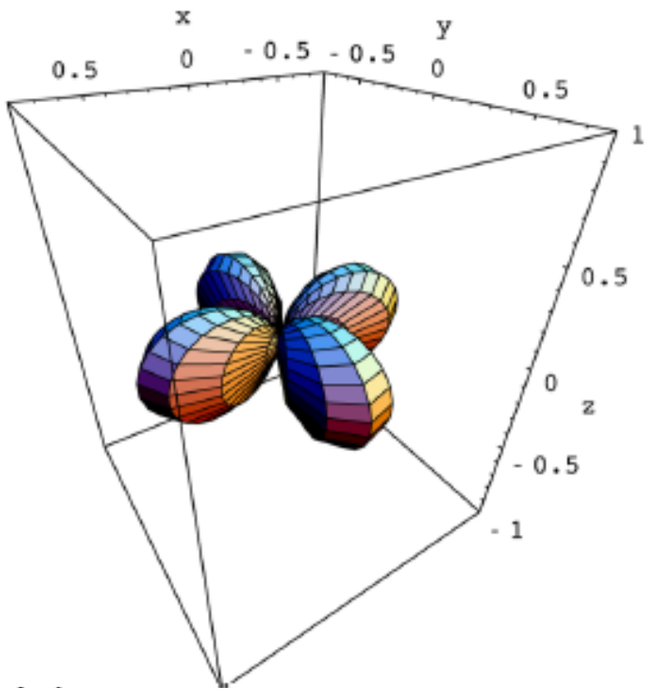

Scalar modes

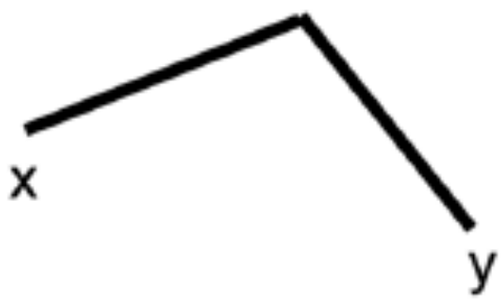

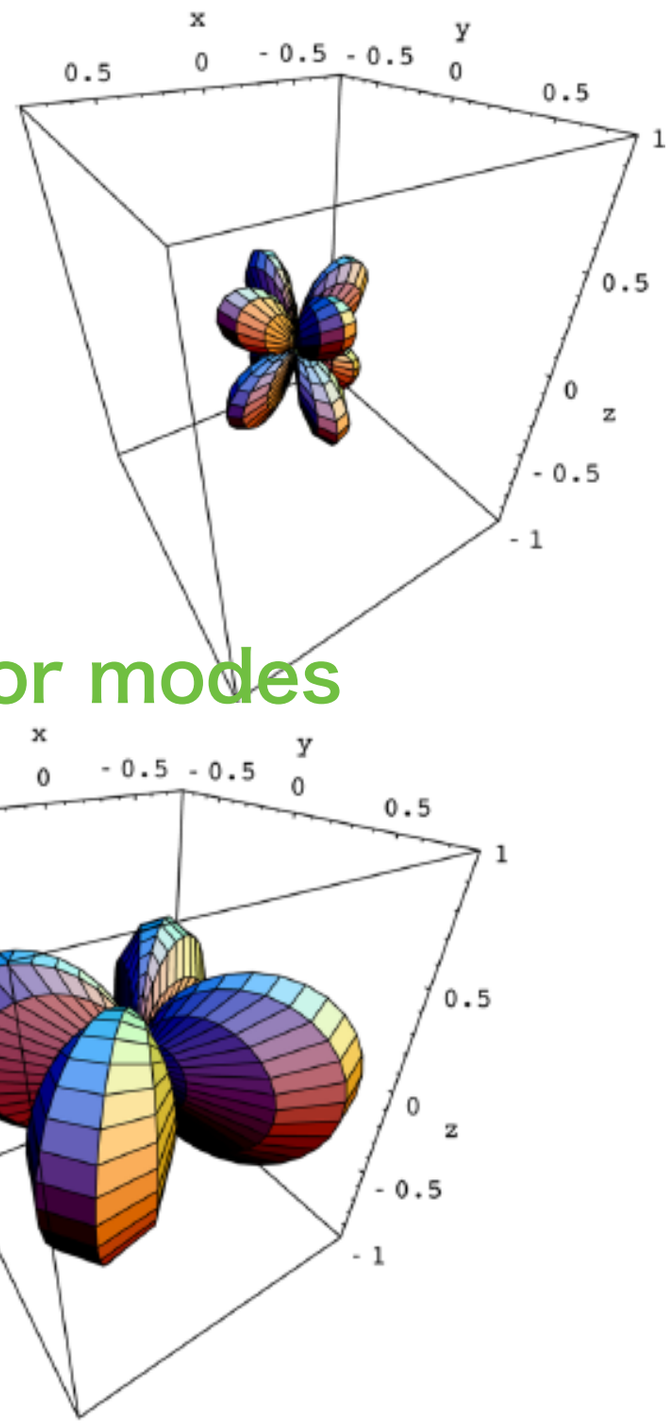

Vector modes

A. Nishizawa et al. PRD 79, 082002 (2009)

How can we detect polarization?

Overlap reduction functions

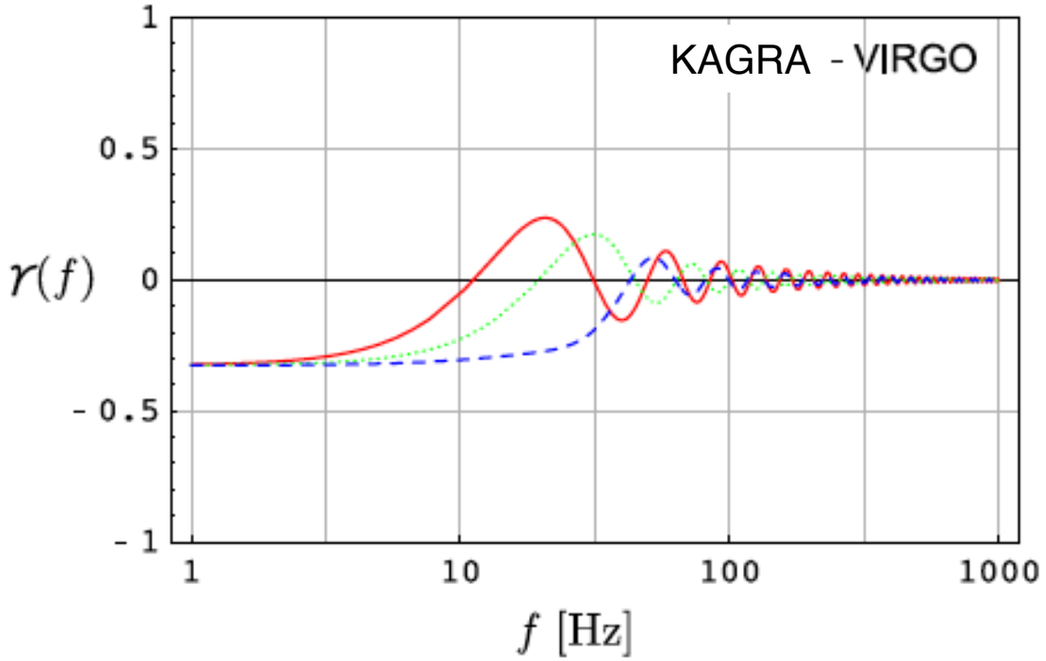

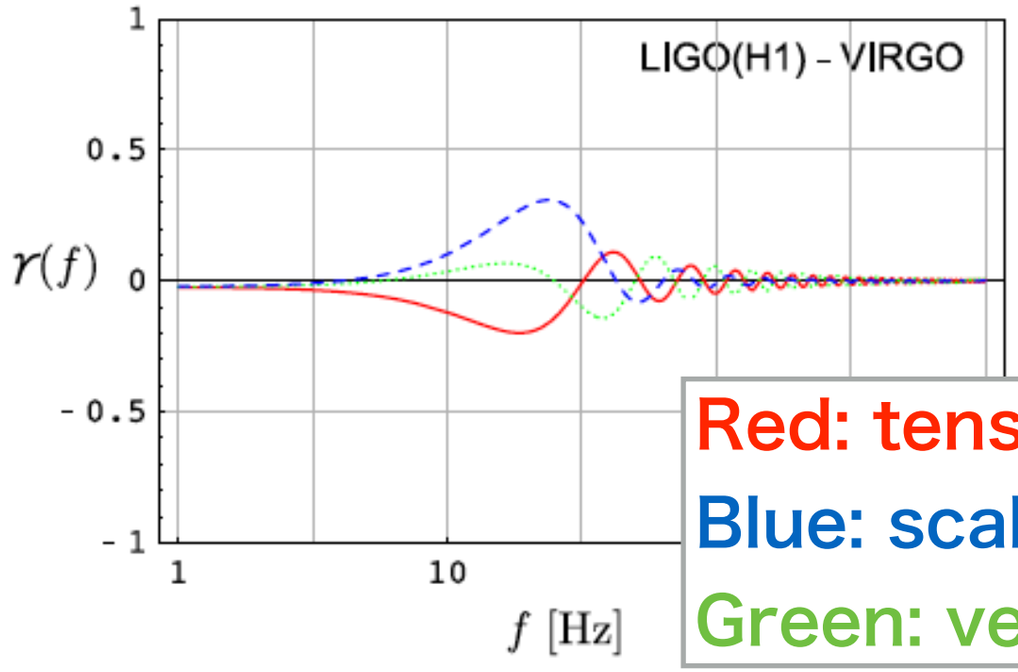

Red: tensor

Blue: scalar

Green: vector

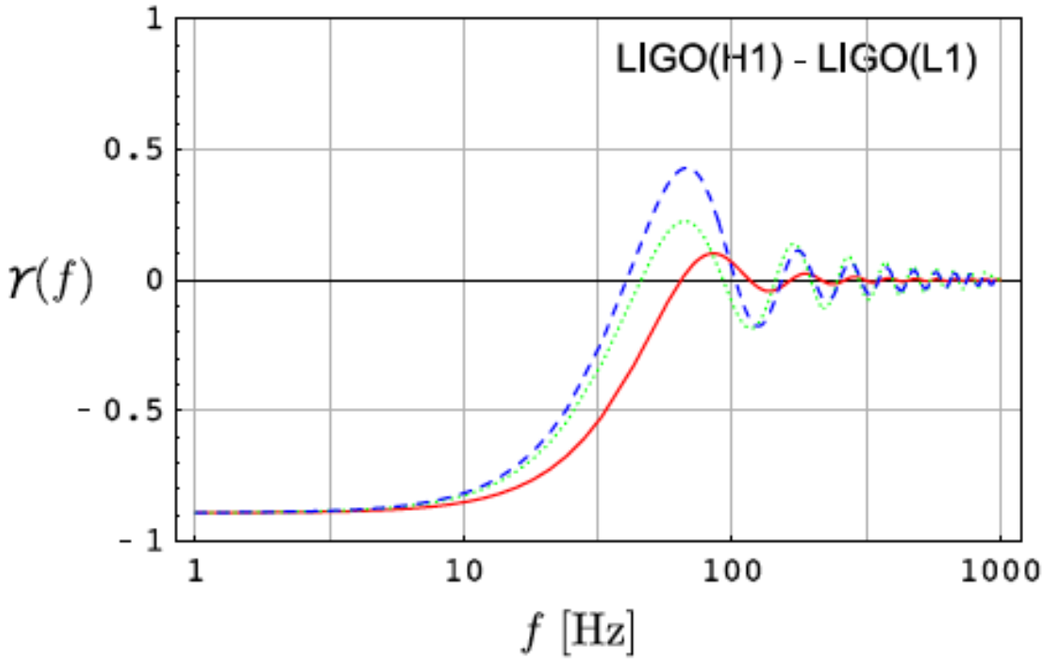

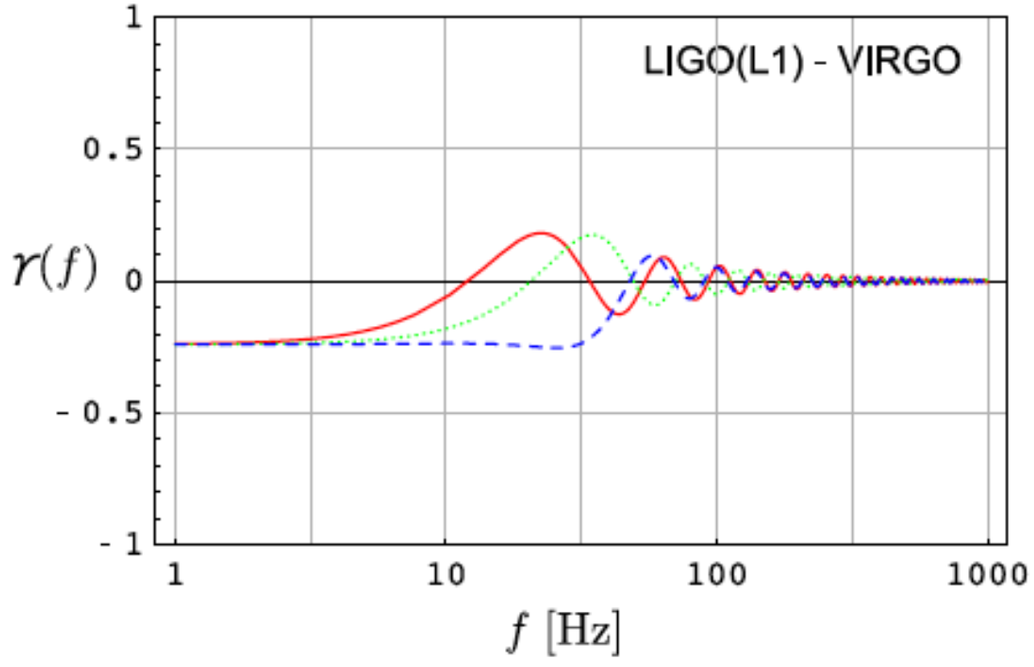

A. Nishizawa et al. PRD 79, 082002 (2009)

How can we detect polarization?

Filter function

overlap reduction function　spectral shape template

$$\tilde{Q}(f) = \lambda \frac{\gamma(|f|)\,\Omega_{\rm gw}(|f|)}{|f|^3 P_1(|f|) P_2(|f|)}$$

noise spectra of detectors

→ We can extract additional polarization modes by changing γ(f)

A. Nishizawa et al. PRD 79, 082002 (2009)

KAGRA will help

O4 sensitivity curves (2021-)

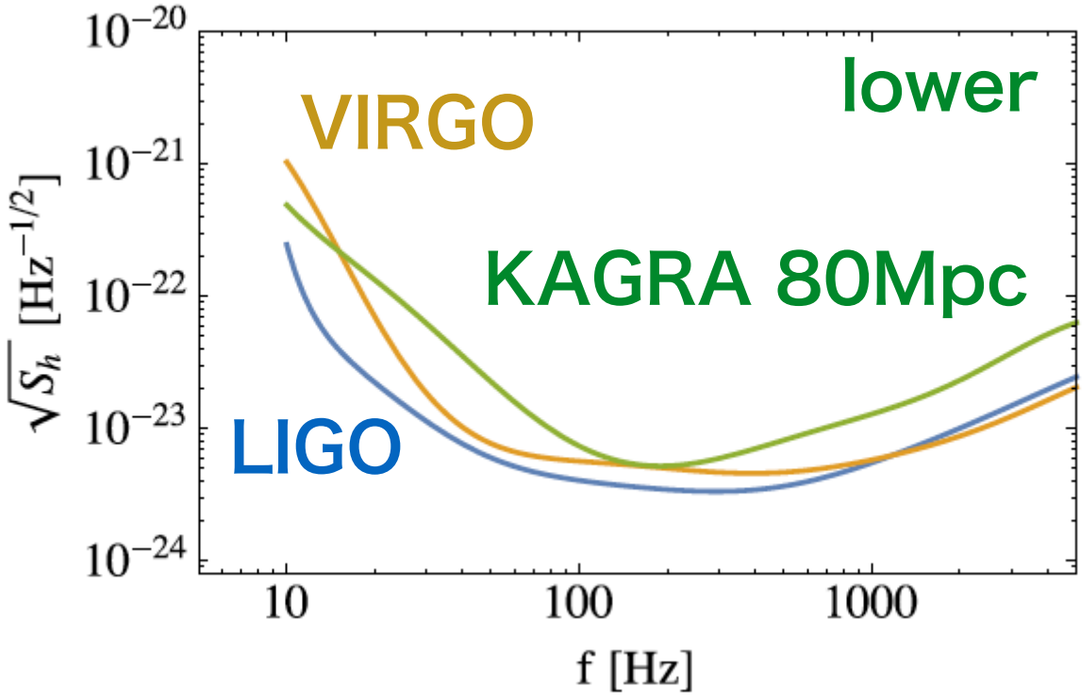

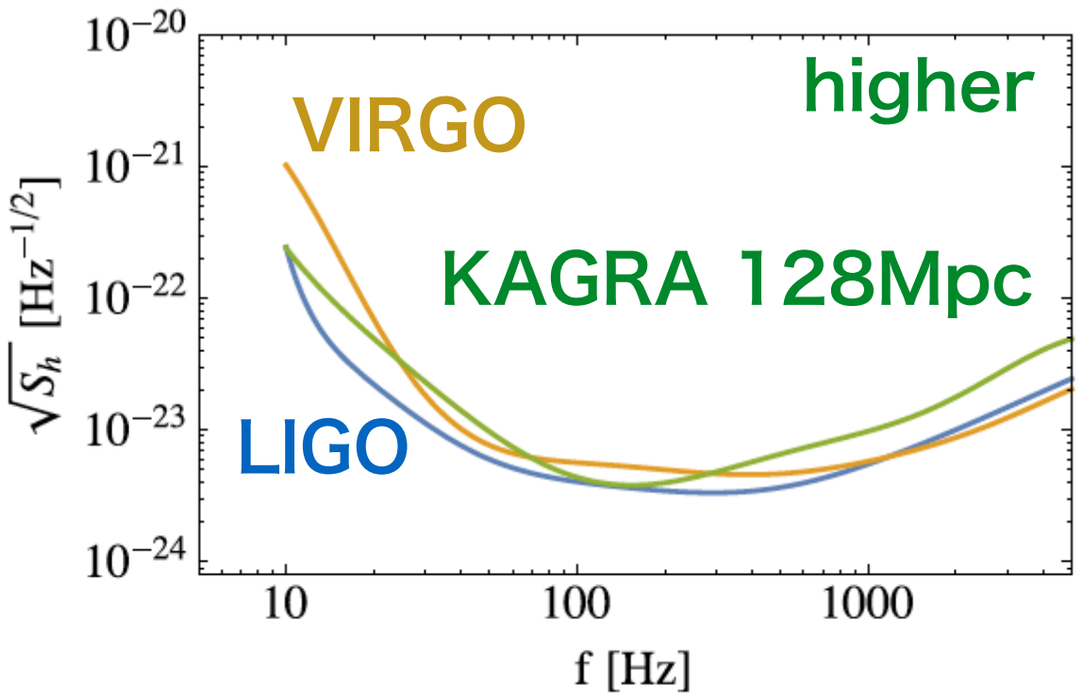

	$\Omega^T_{\rm GW}$	$\Omega^V_{\rm GW}$	$\xi\Omega^S_{\rm GW}$
LIGO×2 + VIRGO	6.6×10^{-9}	1.7×10^{-8}	8.3×10^{-9}
+ KAGRA (80pc)	1.3×10^{-8}	2.1×10^{-8}	1.4×10^{-8}
+ KAGRA (128pc)	5.8×10^{-9}	9.5×10^{-9}	6.6×10^{-9}

ongoing work with A. Nishizawa & G. Liu (KAGRA collaboration)

3. Anisotropy

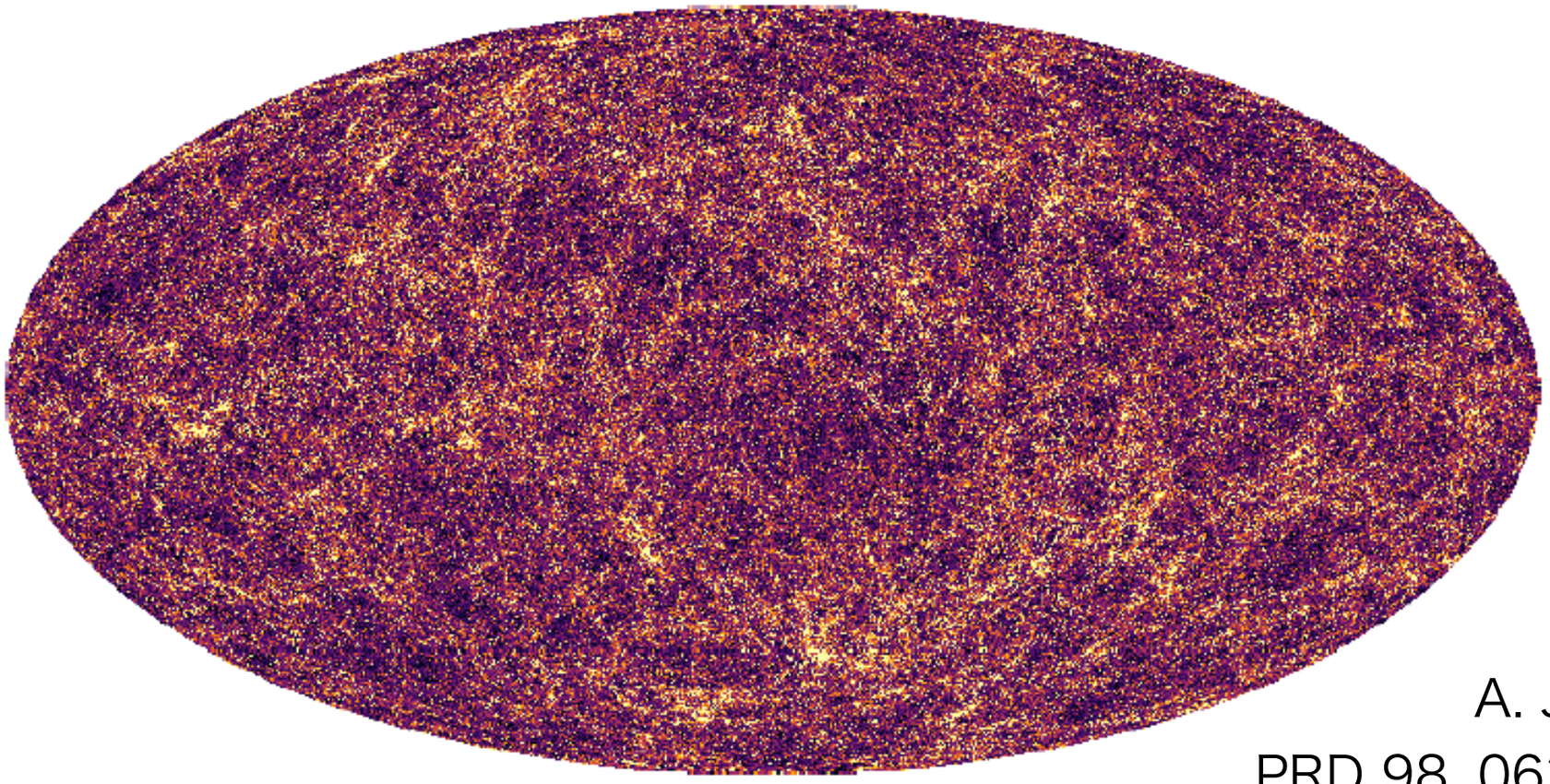

A. Jenkins et al.
PRD 98, 063501 (2018)

Anisotropy of BBH GW background

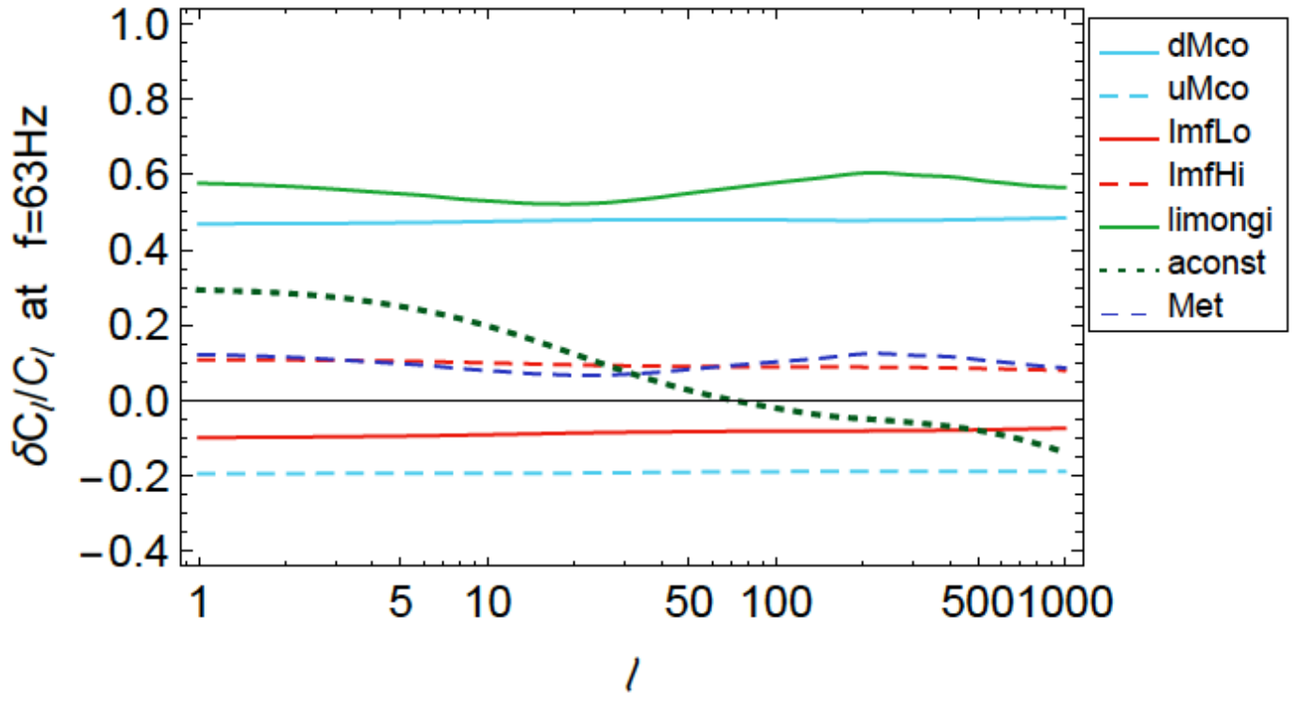

G. Cusin et al., arXiv:1904.07757 [astro-ph.CO]

→ helpful to distinguish between astrophysical and cosmological origin

How can we detect anisotropy?

Overlap reduction function changes

$$\gamma_{IJ}^{T}(f) \equiv \frac{5}{2}\int_{S^2}\frac{d\hat{\mathbf{\Omega}}}{4\pi}e^{2\pi i f\hat{\Omega}\cdot\Delta\vec{X}/c}(F_I^+F_J^+ + F_I^\times F_J^\times)$$

isotropic GWs integrated over the whole sky

1. Radiometry

S. W. Ballmer, CQG 23, S179 (2006)

$$\gamma_{IJ}^{\hat{\mathbf{\Omega}}} \equiv \frac{1}{2}e^{2\pi i f\hat{\mathbf{\Omega}}\cdot\Delta\vec{X}/c}(F_I^+F_J^+ + F_I^\times F_J^\times)$$

→ filter for a point source in direction $\hat{\mathbf{\Omega}}$

2. Spherical harmonics

B. Allen & A. C. Ottewell, PRD 56, 545 (1997)
E. Thrane, PRD 80, 122002 (2009)

$$\gamma_{IJ,lm} \equiv \frac{1}{2}\int d\hat{\mathbf{\Omega}}\; Y_{lm}(\hat{\mathbf{\Omega}})e^{2\pi i f\hat{\mathbf{\Omega}}\cdot\Delta\vec{X}/c}(F_I^+F_J^+ + F_I^\times F_J^\times)$$

→ optimized for extended sources

4. Popcorn noise

Non-overlapping GW bursts

E. Thrane, PRD 87, 043009 (2013)

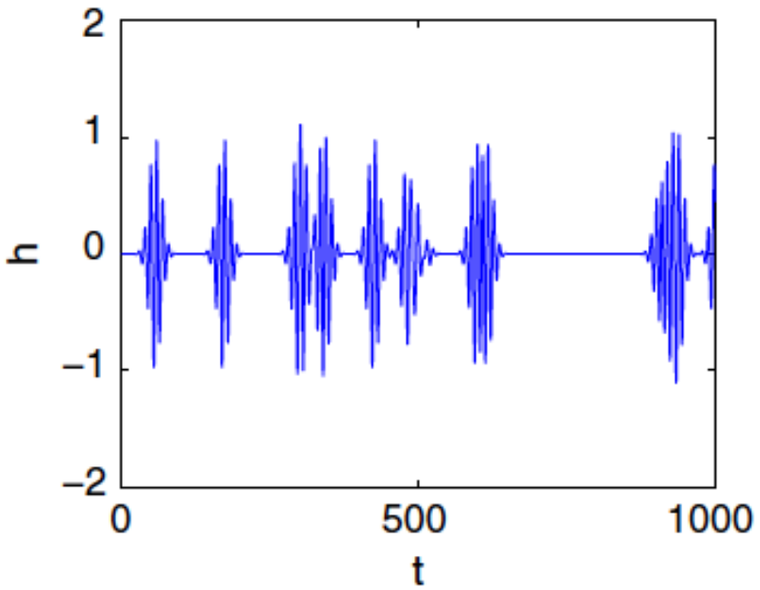

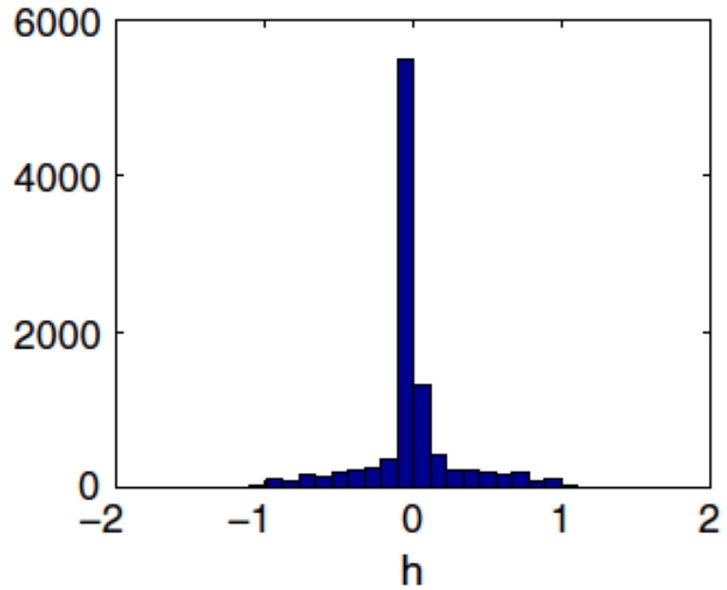

non-Gaussian distribution

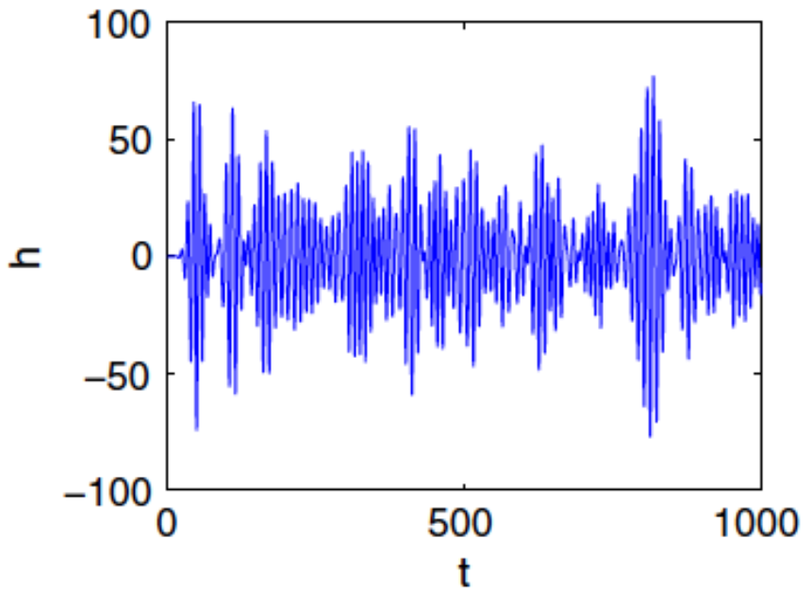

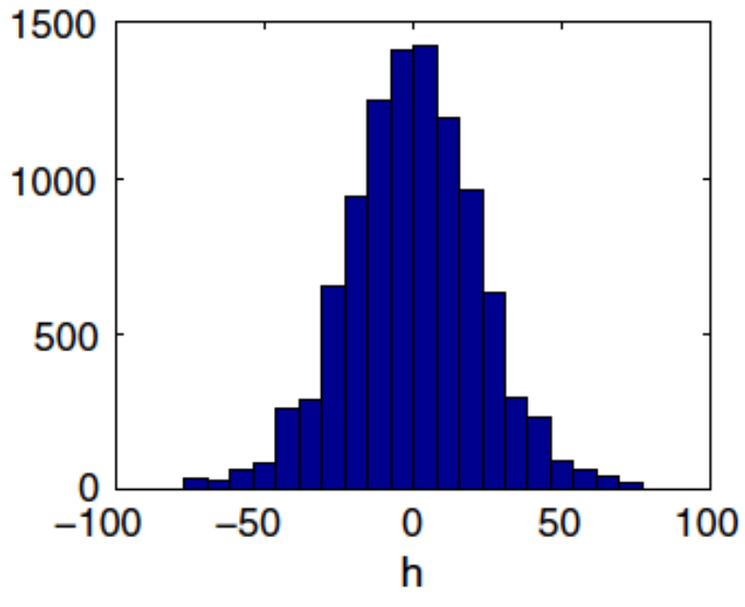

Gaussian distribution

→ helpful to distinguish between astrophysical and cosmological origin

5. Non-Gaussianity

$$\left\langle h_{\lambda_1}\left(t,\,\vec{k}_1\right) h_{\lambda_2}\left(t,\,\vec{k}_2\right) h_{\lambda_3}\left(t,\,\vec{k}_3\right)\right\rangle = \delta^{(3)}\left(\vec{k}_1+\vec{k}_2+\vec{k}_3\right)\mathcal{B}_{\lambda_1,\lambda_2,\lambda_3}\left(\vec{k}_1,\vec{k}_2,\vec{k}_3\right)$$

- Overlapped astrophysical sources
- Sub-horizon produced cosmological GWs

(Phase transitions, Preheating, etc…)

→ **Gaussian (the central limit theorem)**

- Inflation
- Topological defects (long strings)

→ **could generate non-Gaussianity**

N. Bartolo et al. (LISA Cosmology Working Group), JCAP 1811 11, 034 (2018)

Summary

Information beyond the amplitude of a GW background

1. Spectral shape → applicable to all origins

2. Polarization → probe of non-GR

3. Anisotropy

4. Popcorn noise

→ typically of astrophysical origin

5. Non-Gaussianity → inflationary models

→ **Hints for discriminating origins**

Once it is detected and the origin is known, it will bring a breakthrough in the understanding of our Universe